Journal of Low Temperature Physics (2022) 209:1151–1157
https://doi.org/10.1007/s10909-022-02821-w

Investigation of Superconducting Molybdenum Silicide Nanostrips and Microstrips for Single Photon Detectors

L. Parlato[1,2] · D. Salvoni[2,3] · M. Ejrnaes[4] · F. Mattioli[5] · A. Gaggero[5] · F. Martini[5] · D. Massarotti[2,6] · D. Montemurro[1] · R. Satariano[1] · R. Ferraiuolo[1] · F. Chianese[1,2] · F. Tafuri[1] · R. Cristiano[4] · G. P. Pepe[1,2]

Received: 29 October 2021 / Accepted: 1 August 2022 / Published online: 5 September 2022

Abstract

Superconducting nanostrip single photon detectors have emerged as the highest performing single-photon detectors; however, the possibility to use superconducting microstrip as single photon detectors is very appealing both to use them as larger areas detectors and for an easier technology in the manufacturing. The aim of this work is to test the photoresponse in liquid helium dewar of 9 nm thick MoSi covered with a very thin (2 nm) layer of Al, in two different configurations: nanomeanders and microstrips. We demonstrate that MoSi/Al microstrips can work as photodetectors also at $T = 4.2$ K. We also compare the dark count rate of the microstrip and the nanowire, confirming the lower noise for the microstrips also at 4.2 K.

Keywords Superconducting single photon detectors · Nano-microstrips · Dark counts

✉ L. Parlato
lparlato@unina.it

[1] Dip. di Fisica, Università degli Studi di Napoli Federico II, 80125 Naples, Italy

[2] CNR-SPIN, Institute of Superconductors, Innovative Materials and Devices, 80126 Naples, Italy

[3] Dip. di Ingegneria Chimica, dei Materiali delle Produzioni Industriali, Università degli Studi di Napoli Federico II, 80125 Naples, Italy

[4] CNR-SPIN Institute of Superconductors, Innovative Materials and Devices, 80078 Pozzuoli, Italy

[5] CNR, Institute for Photonics and Nanotechnologies, 00156 Rome, Italy

[6] Dip. di Ingegneria Elettrica e delle Tecnologie dell'Informazione, Università degli Studi di Napoli Federico II, 80125 Naples, Italy

1 Introduction

Superconducting nanostrip single photon detectors (SNSPDs) have emerged as the highest performing single-photon detectors due to near-unity efficiency in the near-infrared band, high count rate (above 100 MHz), dark count rates (DCR) lower than 10^{-1} cps, and low timing jitter (3 ps) [1]. Recent developments in SNSPD technology have enabled single photon detection at much longer wavelengths extending into the mid-infrared. This opens the possibility for new applications in molecular science [2–4], in the dark matter search [5], infrared LIDAR technique [6]. Other applications should also gain benefits from the use of large area detectors. In the latter case, instead of SNSPDs with 100 nm-wide strip and which are affected by a significant increase in the kinetic inductance, a better solution may be to resort in the use of superconducting microstrip single photon detectors (SMSPDs) [7, 8]. The performances of these detectors depend on the materials properties, design, fabrication process, and measurement conditions. Different superconducting materials have been used as SNPSDs. Typically, NbN or NbTiN operating around 2 K have been employed [2, 9]. Many other conventional [1] or unconventional materials have been tested such as: NbRe [10], MgB_2 [7], YBCO [11], or hybrid structures [12, 13]. Even more challenging is the idea of implementing iron-based materials that show very slow thermalization time [14]. Superconducting materials based on amorphous materials, such as WSi [15], MoSi [16], having low energy gap, high uniformity and resistivity, have been demonstrated to be an interesting alternative. Recently, photon detection with micron-wide strips has been demonstrated [17–19] and theoretically predicted [20]. The model, based on numerical solution of time-dependent Ginzburg–Landau equations, predicts that if the bias current is close enough to the depairing current I_{dep}, the photon absorption leads to the formation of vortex-antivortex pairs in the hot-spot. Movement of the vortices leads to the Joule heating of the strip and destruction of superconductivity.

Another important feature of SN/MSPDs is their low DCR that increases close to the critical current where the detection efficiency is higher. In such a region DCR is dominated by a spontaneous resistive-state formation, i.e., an intrinsic decoherent phenomenon occurring in superconducting strips. The investigation of the origin of DCR toward optimization of SN/MSPD's performances is crucial.

In this work, we explore the photoresponse at $\lambda = 1550$ nm and the dark counts in a liquid helium dewar at 4.2 K of a 9 nm thick MoSi covered with a very thin (2 nm) layer of Al, in two different configurations: nanomeanders 140 nm wide, previously demonstrated to work as single photon detector [21], and microstrips 2 μm wide. We observe that also the 9 nm thick MoSi/Al microstrip presents a good signal-to-noise ratio at 4.2 K, making these samples good candidates to be used as single photon detectors in liquid helium. Better performances could be achieved by lowering the temperature and the thickness of the superconducting film, but the purpose of this work is to explore the performance of these novel devices in transport liquid helium dewar, which can be particularly favorable for some on field applications when the cooling time of a closed cycle cryostat can be prohibitive. A comparison of the dark count rates for the two geometries is also presented.

2 Fabrication

$Mo_{0.70}Si_{0.30}$ films, 9 nm thick, have been deposited on Si/SiO_x (250 nm) substrate by dc magnetron sputtering at a rate of 0.2 nm/s at room temperature. Immediately after and without vacuum breaking, 2 nm of Al have been deposited at a rate of 0.3 nm/s, to protect the superconducting material during the patterning of the film and prevent the oxidation of the MoSi surface. The thickness of the films is estimated by the deposition time and deposition rate. The latter is measured in a calibration process when thick film is deposited. Reasonably, the 2 nm Al film is completely oxidized when the sample is extracted from the vacuum chamber. The critical temperature of a 9 nm thick MoSi film covered by the Al, estimated by the middle of $R(T)$ curve, is $T_c = 6.5$ K opening to the possibility to work at 4.2 K. The films have been patterned by using electron beam lithography (EBL) and reactive ion etching (RIE) realizing nanomeanders of nominal widths from 150 nm down to 100 nm, covering a square area of 5 μm × 5 μm (Fig. 1). Single microstrips with width from 2 μm up to 5 μm with different length ranging from 5 μm up to 25 μm has been fabricated by using electron beam lithography (EBL) and lift off technique [22, 23] (Fig. 1 right). The widths have been chosen to match what can be reliably realized with conventional photolithographic techniques.

The entry and exit points of the strips and turns of the meanders have rounded edges, as shown in Fig. 1, to prevent current crowding effects [24].

3 Measurements

All the fabricated samples are first tested at 4.2 K measuring IV-curves. We measured several strips for each width and successively selected the samples with the highest critical currents for further investigation. Typical current–voltage characteristics for a MoSi/Al nanomeander 140 nm wide, measured at 4.2 K and 1.3 K, respectively, are shown in the left panel of Fig. 2. At both temperatures, as the bias current is swept from zero to higher values of current the strip exhibits an abrupt transition from the superconducting state (zero voltage) to a finite voltage state.

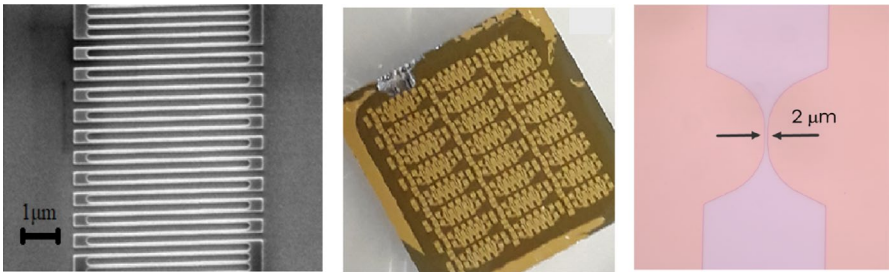

Fig. 1 *Left:* SEM image of a MoSi/Al SNSPD, 140 nm wide, 9 nm thick and 100 μm long; *Center*: View of the chip with 3 × 8 devices with nanomeander of different width; *Right*: Microscope image of a MoSi/Al SMPD, 2 μm wide, 9 nm thick and 10 μm long. (Color figure online)

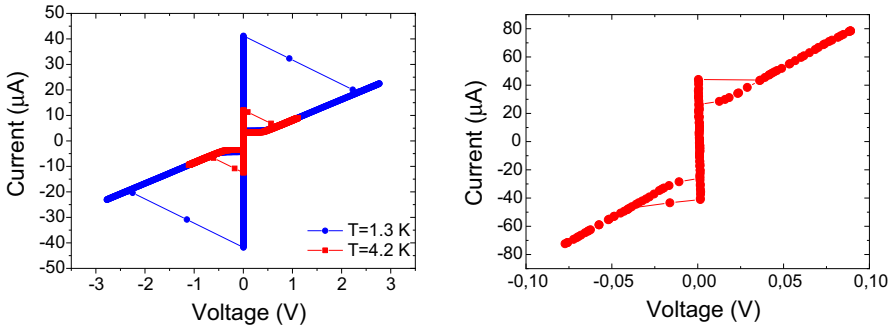

Fig. 2 *Left*: Current–voltage characteristics of a nanomeander 140 nm wide at $T=1.3$ K (*blue circle symbols*) and $T=4.2$ K (*red square symbols*), respectively. *Rigth:* Current–voltage characteristic of a microstrip 2 μm wide at $T=4.2$ K. (Color figure online)

The abrupt current suppression is caused by the high normal resistance value of the nanomeander. The strip will stay in the finite voltage state until the current is reduced below the re-trapping current at which point the strip becomes superconducting again. The average critical current densities J_c are 3.2 MA/cm^2 and 0.8 MA/cm^2 at $T=1.3$ K and $T=4.2$ K, respectively. We observe that the IV curves are hysteretic also at $T=4.2$ K without a deterioration of the superconducting properties (critical current, critical temperature, etc.) with the time, probably due to the presence of the fully oxidized Al coverlayer. The hysteresis in the IV curve is a key feature in SN/MSPDs since the voltage pulse arising after a photon detection is proportional to its amplitude. The presence of a sharp hysteresis in some of the fabricated MoSi/Al strips even at 4.2 K guarantees the possibility to perform photon counting also inside a liquid helium dewar. We observe a lower critical current density in the case of our microstrips with respect to nanostrips ($J_c=0.2$ MA/cm^2 at $T=4.2$ K, and it differs from each other device by about 10%).

Since the microstrip detectors present smaller kinetic inductance, they are more affected by *latching*, i.e., the superconducting regime does not spontaneously restore after the switching event. For this reason, an additional inductance (470 nH) and a shunt resistor (100 Ω) are mounted, producing a rise-time $\tau_{rs}=6$ ns and a fall-time $\tau_f=27$ ns.

We have measured the DCR as a function of the bias current for both nano- and microstrips (Fig. 3). We observe that the DCR increases exponentially by increasing the bias current up to the critical current. However, in the case of the microstrips the DCR is lower with respect to the nanostrips, as observed in the literature [17], and they decrease faster as the bias current decreases. This means that there is an extended bias current range where the DCR is at least three orders of magnitudes higher for the nanostrips with respect to the microstrips. Geometrical, superconducting, electrical properties and DCR of devices under study are summarized in Table 1.

This behavior can be ascribed to the vortex mechanisms probably responsible of the fluctuation events and then of the dark counts [25–27]. Magnetic vortices moving across the width of a superconducting strip, either vortex antivortex pairs (VAP)

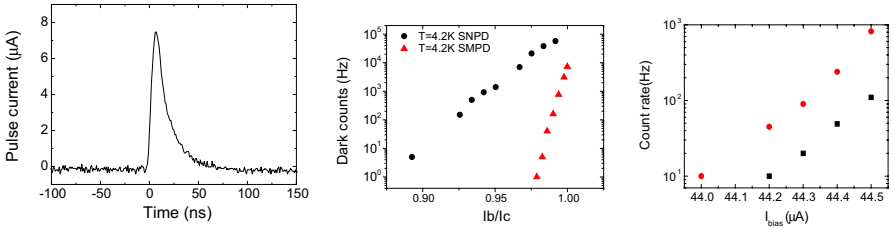

Fig. 3 *Left*: Measured dark pulse at $T=4.2$ K when a strip 2 μm wide and 10 μm long was biased close to the critical current (the nanostrip pulse measured with different electronics can be found in [21]). *Center:* DCR vs normalized current at $T=4.2$ K for a nanomeander (*dark circle points*) and a microstrip (*red triangular points*). *Right*: the photoresponse at $\lambda=1550$ nm (red circular points) and DCR (*square dark points*) vs bias current at $T=4.2$ K for a 2 μm wide and 10 μm long microstrip. (Color figure online)

Table 1 Geometrical, superconducting, electrical properties and response of devices under study

Sample	w (μm)	R_S (Ω/sq)	$J_{c@\ T=4.2\,K}$ (MA/cm^2)	$DCR_{@\ T=4.2\,K}$ (Hz)	Process
Nanomeander	0.09	250	0.5	N.a	RIE
Nanomeander	0.14	185	0.8	57,000	RIE
Microstrip	2	190	0.2	770	Lift off
Microstrip	5	670	0.2	N.a	Lift off

w is the width of the devices, R_S the square resistance in the normal state, J_c the density current at $T=4.2$ K, DCR the dark count rate at $I_b/I_c=0.99$

Table 2 Photoresponse at 1550 nm of devices under study

Sample	w (μm)	T (K)	I_b/I_c	PCR/DCR	Single photon response
Nanomeander	0.14	3.0	0.90	718	Yes
Microstrip	2	4.2	0.99	5	Unknown

or as single vortices (SV) overcoming the barrier at opposite edges of the strip, play a relevant role. Indeed, the binding energy of the VAP and SV is significantly lower (about one order of magnitude) in the case of narrowest strips favoring the spontaneous fluctuation events without the absorption of an external photon. The rate of single vortices entering the strip is proportional to the length L of the strip whereas the rate of VAP break-up is proportional to the area (Lw) of the superconducting film [25]. Therefore, the ratio of VAP to SV rates is supposed to be proportional to the strip width w and one can expect that VAP events start to dominate in wider strips.

Finally, we illuminated the devices with an optical fiber at $\lambda=1550$ nm (see Table 2). The distance between the device and a standard single mode SMF 28 fiber is about 1 cm, providing a uniform illumination on the detector area. The single photon detection regime was already demonstrated in [21] for the nanomeanders. In Fig. 3 (*right*) we report on the photoresponse for a microstrip 2 μm wide. It is

seen that the photoresponse counting rate increases above the dark count rate. The increase is below one order of magnitude which is not sufficient for determining if this response is a single photon response with the usual light attenuation technique. Furthermore, we do not observe any saturation effect at high bias currents close to the critical current, as also observed in [28] for wider stripes.

4 Conclusion

We have realized 9 nm thick MoSi covered with a very thin (2 nm) layer of Al to raise the T_c, in two different configurations: nanomeanders and microstrips. We observe a current hysteresis in the I–V curves at $T = 4.2$ K also for the samples below 2 μm wide. For these samples, we investigate the dark counts events and observe a photoresponse in a liquid helium dewar. The possibility to use microstrips is very appealing both to use them as large areas detectors and to ease the manufacturing. Moreover, working in liquid helium transport dewar can facilitate the operation for some applications.

Acknowledgements The authors thank Prof. A. Cassinese and the national project PON E-Design (ARS01_01158), funded by the Italian Ministry of Education, University and Research (MIUR). The activities have received funding from the European Unions Horizon 2020 research and innovation programme under Grant Agreement No 654109, ACTRIS2 project.

Funding Open access funding provided by Università degli Studi di Napoli Federico II within the CRUI-CARE Agreement.

Data availability Data will be made available on the reasonable request.

References

1. L. You, Nanophotonics **9**(9), 2673–2692 (2020)
2. W. Zhang et al., Phys. Rev. Appl. **12**(4), 044040 (2019)
3. D. Salvoni et al., J. Phys. **1182**(1), 012014 (2019)
4. G. Taylor et al., Opt. Express **27**(26), 38147–38158 (2019)
5. Y. Hochberg et al., Phys. Rev. Lett. **123**, 151802 (2019)
6. D. Salvoni et al., Chem. Eng. Trans. **84**, 175–180 (2021)
7. S. Cherednichenko et al., Supercond. Sci. Technol. **34**, 044001 (2021). https://doi.org/10.1088/1361-6668/abdeda
8. X. Zhang et al., Supercond. Sci. Technol. **34**, 095003 (2021). https://doi.org/10.1088/1361-6668/ac1524
9. F. Marsili et al., Nano Lett. **12**, 4799–5480 (2012)

10. C. Cirillo et al., Appl. Phys. Lett. **117**, 172602 (2020)
11. M. Ejrnaes et al., Supercond. Sci. Technol. **30**(12), 12lt02 (2017)
12. G.P. Pepe et al., Cryogenics **49**, 660 (2009)
13. C. Cirillo et al., Phys. Rev. B **84**(5), 054536 (2011)
14. C. Bonavolontà et al., Supercond. Sci. Technol. **26**, 075018 (2013)
15. F. Marsili et al., Nat. Photonics **7**(3), 210–214 (2013)
16. V.B. Verma et al., Opt. Express **23**(26), 33792–33801 (2015)
17. Y.P. Korneeva et al., Phys. Rev. Appl. **9**, 064037 (2018)
18. I. Charaev et al., Appl. Phys. Lett. **116**, 242603 (2020)
19. J. Chiles et al., Appl. Phys. Lett. **116**, 242602 (2020)
20. D.Y. Vodolazov, Phys. Rev. Appl. **7**, 034014 (2017)
21. D. Salvoni et al., IEEE Inst. Meas. Mag. **24**, 69 (2021). https://doi.org/10.1109/MIM.2021.9491006
22. D. Montemurro et al., Nanotechnology **26**(38), 385302 (2015)
23. E. Trabaldo et al., Appl. Phys. Lett. **116**(13), 132601 (2020)
24. J.R. Clem, K.K. Berggren, Phys. Rev. B **84**, 174510 (2011)
25. H. Bartolf et al., Phys. Rev. B **81**, 024502 (2010)
26. L. Parlato et al., J. Low Temp. Phys. 1–6 (2020)
27. M. Ejrnaes et al., Sci. Rep. **9**(1), 1–6 (2019)
28. Y.P. Koorneva et al., Supercond. Sci. Technol. **34**, 084001 (2021)